Study on development policy for new cryogenic structural material for superconducting magnet of fusion reactor

Nuclear Materials and Energy 30 (2022) 101125

Contents lists available at ScienceDirect

Nuclear Materials and Energy

journal homepage: www.elsevier.com/locate/nme

Study on development policy for new cryogenic structural material for superconducting magnet of fusion reactor

Arata Nishimura [a,*], Yoshinori Ono [b], Osamu Umezawa [c], Susumu Kumagai [d], Yohko Kato [c], Tetsuya Kato [c], Tetsumi Yuri [b], Masayuki Komatsu [b]

[a] National Institute for Fusion Science, Japan
[b] National Institute for Materials Science, Japan
[c] Yokohama National University, Japan
[d] National Institute of Technology, Sendai College, Japan

ARTICLE INFO

Keywords:
Cryogenic structural material
Fusion DEMO
Hall-Petch diagram
Fracture toughness
Huge component

ABSTRACT

A fusion DEMO will require large-scale cryogenic structure including TF coil cases. Because of huge electromagnetic forces, extra thick plates and/or wrought products will be supplied. Since the midsection of the huge block is weaker than the block surface region, the design yield stress must be determined taking account of this lower strength part. To search the manufacturing process to improve the midsection strength, the crystal refinement strengthening and the precipitation strengthening are considered together with the carbon and nitrogen solid solution strengthening. XM-19 was focused based on the variation of the yield stress and the fracture toughness, a 100 mm thick block and a 30 mm thick plate were trial produced, and strength and the fracture toughness at the midsection were evaluated. This study will present the experimental data and discuss the development policy for a new cryogenic structural material for a fusion reactor.

1. Introduction

The ITER project [1] is undergoing, and a fusion DEMO project will follow the ITER. Japan and European fusion communities have published the plans of JA DEMO [2] and EU DEMO [3]. The Major radius, the fusion output, the plasma current, and the magnetic field on plasma axis of the ITER, JA DEMO and EU DEMO are 6.2, 8.5 and 9.0 m, and 0.5, 1.46 and 2.0 GW, and 15, 12.3 and 18 MA, and 5.3, 5.94 and 5.9 T, respectively. Therefore, the DEMO will be about 1.5 times larger than the ITER, and the total weight of the DEMO will become about 78,000 tons, when the global density of the fusion reactor is assumed as the same as the ITER and the weight of the ITER is about 23,000 tons [4].

The higher magnetic field improves the plasma confinement, and high temperature superconducting (HTS) tapes can provide the higher magnetic field. In case of SPARC undergoing at MIT and Commonwealth Fusion Systems in US, the magnetic field at the plasma axis is about 12 T and the maximum field in the TF coil reaches over 20 T. The toroidal field (TF) model coil test has been done successfully in September 2021 [5,6].

Therefore, the higher strength and the thicker structural materials must be developed for the fusion reactor. Several new cryogenic structural materials have been developed in Japan, and about 400 mm thick blocks were produced during the R&Ds for the ITER TF magnet in 1980s to 1990s [7,8]. Nowadays, over 1200 MPa of the design yield stress is expected to be developed for the JA fusion DEMO [2].

In 1970 s, lots of works on austenitic stainless steel, mainly 304 and 316, were performed, and the parameter of carbon plus nitrogen content, (C + N) in mass %, was found to present the strength at 4 K. When (C + N) increases, the yield strength improves. Both elements are diffusional, and the solid solution strengthening was confirmed [9]. In case of the huge fusion reactor, very thick plates or large blocks are required to support the huge electromagnetic force. Generally, the midsection part of the large block is weaker than the surface part, for the strain hardening does not occur enough like the surface part during forging and rolling. Because of this lower yield strength, the design yield stress of the cryogenic structural material is set in a lower level. If the midsection part of the large wrought products could show the same strength as the surface part, the design yield stress can be increased, and rather compact structure could be designed. At the same time, the structural material can be saved, which is very important for production.

* Corresponding author.
E-mail address: nishimura.arata@toki-fs.jp (A. Nishimura).

https://doi.org/10.1016/j.nme.2022.101125
Received 29 October 2021; Received in revised form 24 December 2021; Accepted 21 January 2022
Available online 25 January 2022

As mentioned above, the TF model coil of SPARC was successfully performed. The magnet was fabricated using HTS tapes and the operation temperature was 20 K. The degree of the reduction of the design yield stress at 4 K to 20 K depends on the material. For one example, JSME SKA1-2013 [10] presents the following equation for Japanese Cryogenic Steel (JCS) JJ1 to give the design yield stress in the range from 300 K to 4 K (thickness < 200 mm):

$$\text{Design yield stress (MPa)} = 0.007975 \times T^2 - 5.030 \times T + 1090 \quad (1)$$

where T is the operation temperature (K). From this equation, the design stresses at 4 K and 20 K can be obtained as 1065 MPa and 993 MPa, respectively, and the reduction ratio becomes about 6.8%. Although the detailed mechanical properties at 20 K must be investigated carefully, it is clear that the extra thick higher strength cryogenic material is desired and must be developed for the fusion reactor.

In this paper, some data at 4 K of the trial-manufactured thick XM-19 will be presented together with the published ones and the direction of the development of the new cryogenic structural material will be discussed focusing on the mechanical properties at the midsection of the extra thick plate or block.

2. Cryogenic structural materials

2.1. Strengthening processes

Traditionally, there are several processes to strengthen the structural materials as follows:

(1) Strain hardening: By introducing the dislocations in the material, the yield stress increases. (2) Solid solution strengthening: Carbon and nitrogen are interstitial solution elements and strengthen the material. (3) Crystal refinement hardening: By making the grains finer, the strength can be improved. Hall-Petch relation was found empirically. (4) Precipitation strengthening: By adding proper elements such as V and Nb, the second phase precipitations will be formed which prevent the dislocation movement resulting in the higher yield stress. (5) Dispersion strengthening: Some larger precipitations or oxides will be formed by the heat treatment and dispersed particles stop the dislocation movement and increase the higher yield stress.

2.2. Chemical compositions of some cryogenic structural materials

The chemical compositions of 316LN in Japan Industrial Standard (JIS) is shown in Table 1 together with the other structural materials for the cryogenic application. 316LN does not contain V and Nb and contains N of 0.22 mass % maximum. The relation between the yield stress in MPa at 4 K and (C + N) in mass % is presented as follows [11,12]. The scatter band is about +/- 150 MPa.

$$\text{For 4K;}\ \sigma_Y = 3300 \times (C + N) + 350 \quad (2)$$

(C + N) will become the maximum of 0.25 mass % and show the yield stress of about over 1000 MPa at 4 K. 90 mm thick data (Alstom) and 700 mm thick data (Alcator CMOD) show the lower yield stress [12]. TF case JJ1 in Table 1 shows the requirements for the ITER TF coil case material. It contains higher Mn, Mo and N and less Cr than those of 316LN. It has the yield stress of over 1000 MPa and the fracture toughness of 200 MPa$\sqrt{m}$. Central solenoid (CS) jacket JK2 is used for the conduit of the CS module conductor. It has a high Mn system and lower Ni content. Both steels contain B to exhibit the smooth deformation property and N to get the solid solution strengthening. They do not contain V and Nb which produce the crystal refinement and the precipitation strengthening. JCS JN1 in Table 1 [7,8] is an example of another cryogenic structural material. This is a high Ni and high Cr stainless steel with high N. In 1980 s, JBK-75 [13] with high Ni and very low N was investigated for a conductor sheath material.

The ITER has six CS modules, and long tie rods were designed to tie up all modules securely [14]. XM-19 was selected due to its high yield stress. The chemical compositions of XM-19 are also shown in Table 1. It contains higher C, Mn and N. And V and Nb are added. This is a big difference from the other materials. As mentioned above, V and Nb demonstrate the crystal refinement and the precipitation strengthening. The N content is also higher than three materials. When the Eq. (2) is applied with (C + N) of 0.46, the maximum yield stress at 4 K becomes ca 1800 MPa. To investigate the effect of the crystal refinement and the precipitation strengthening to improve the yield stress at the midsection of the extra thick plate, three different XM-19 were trial manufactured [15] as shown in Table 1.

Two ingots of about 180 kg were prepared. One ingot was hot-forged into 150 mm thick block and hot-rolled to 30 mm thick plate (XM-19 #1). The solution heat treatment was carried out at 1373 K for 21.6 ks followed by water quench (WQ). The second ingot was hot-forged into 150 mm thick block and hot-rolled to 100 mm thick block (XM-19 #2). The block was solution heat treated at 1373 K, 1423 K or 1473 K for 21.6 ks followed by WQ. The apparatus of both materials is shown in Fig. 1 for #1 and Fig. 2 for #2. The third (XM-19 #3) was a bar with 30 mm square cross section and cold-rolled to a bar with 14.3 mm square to investigate the grain size effect on the yield stress. The cold-rolled bars were annealed at 1273 K, 1373 K or 1473 K for 3.6 ks followed by WQ. #3 had about half contents of C, V and Nb comparing with #1 and #2, and those V and Nb contents were almost the lowest limit of the XM-19 standard.

The average grain size of the heat-treated materials are as follows (the min. and max. grain sizes are written in parentheses): 20.0 μm (no record) on 1/2 and 1/4 thickness sections of #1. 26.0 μm (21.7, 29.3) at

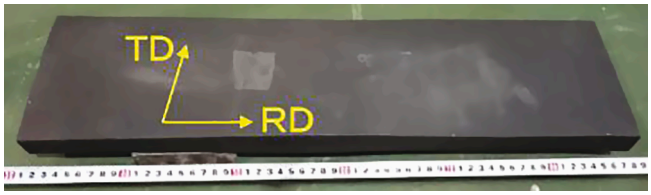

Fig. 1. XM-19 #1 plate. ($30^{t} \times 150^{W} \times 600^{L}$).

Table 1
Chemical compositions of the materials for cryogenic application of fusion devices.

Material	C	Si	Mn	P	S	Ni	Cr	Mo	V	Nb	N	Others
JIS 316LN	≦0.030	≦1.00	≦2.00	≦0.045	≦0.030	10.50–14.50	16.50–18.50	2.00–3.00	–	–	0.12–0.22	
TF case JJ1	≦0.03	≦1.00	9.0–11.0	≦0.040	≦0.010	10.0–13.0	11.0–13.0	4.5–5.5	–	–	0.21–0.27	~10 ppm B
CS jacket JK2	≦0.025	≦0.5	20.5–22.5	≦0.015	≦0.015	8.0–10.0	12.0–14.0	0.5–1.5	–	–	0.09–0.15	10–40 ppm B
JCS JN1	0.026	0.99	4.2	0.026	0.002	14.74	24.2	–	–	–	0.34	
JBK-75	0.018	0.06	0.03	0.002	0.003	30.40	14.70	1.20	0.32	–	0.003	Ti:2.20 B:0.0030
XM-19 ASTM A240	≦0.060	≦0.75	4.0–6.0	≦0.040	≦0.030	11.5–13.5	20.5–23.5	1.50–3.00	0.10–0.30	0.10–0.30	0.20–0.40	
XM-19 #1	0.029	0.410	4.56	0.016	0.002	12.31	21.91	2.11	0.21	0.19	0.329	
XM-19 #2	0.031	0.390	4.53	0.015	0.002	12.26	21.95	2.11	0.20	0.200	0.330	
XM-19 #3	0.015	0.430	5.47	0.016	0.002	13.32	21.82	1.82	0.11	0.100	0.291	

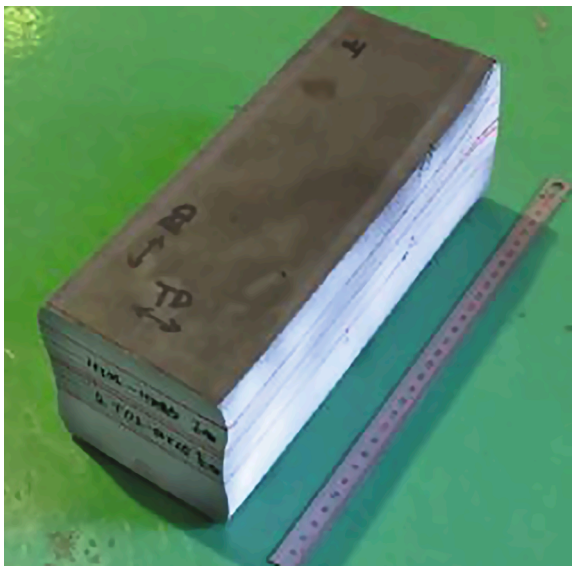

Fig. 2. XM-19 #2 100 mm^{t} block.

1373 K, 41.2 μm (31.0, 48.0) at 1423 K, and 50.3 μm (42.3, 57.5) at 1473 K on 1/2 thickness section of #2, and 24.3 μm (21.6, 29.0) at 1373 K, 45.8 μm (41.1, 48.2) at 1423 K, 59.0 μm (50.6, 67.9) at 1473 K on 1/4 thickness section of #2. 8.9 μm (7,6 11.7) at 1273 K, 42.5 μm (35.2, 51.8) at 1373 K, 147.5 μm (133.0, 167.2) at 1473 K of #3.

3. Test procedures

The tensile tests were carried out according to JIS Z 2277 at 4 K using a round bar specimen with 6.25 mm diameter which was machined out in parallel with the transverse direction (TD) to the rolling direction. The gage length was 31.25 mm, and the crosshead speed was 0.5 mm/min. The fracture toughness tests were performed following ASTM E 1820–11 at 4 K with a half inch CT specimen. The initial notch was induced in the rolling direction and loaded in the transverse direction (T-L specimen). The side grooves were not machined.

Three specimens were tested for each test condition and the average value was used for the discussion.

The fracture surfaces of the tensile specimens and the CT specimens were investigated by SEM and EDX.

4. Results and discussion

4.1. Segregation of Nb

The average elongation at 4 K of each test condition is as follows: 28 and 30 % for 1/2 and 1/4 thickness section of #1 (1373 K). 12 and 15 % for 1/2 and 1/4 thickness section of #2 (1373 K). 14 and 16 % for 1/2 and 1/4 thickness section of #2 (1423 K). 16 and 18 % for 1/2 and 1/4 thickness section of #2 (1473 K). 14 and 16 % for 1/2 and 1/4 thickness section of #2 (1423 K). All specimens showed the serration during the tensile test, and there is possibility that the elongation varies depending on the stiffness of the test machine system.

Prior to this study, the trial investigation was carried out using different XM-19 which contained almost same chemical compositions as XM-19 #1 and #2. The tensile test at 4 K was carried out in transverse direction. The specimen was taken out of on 1/2 thickness section of 100 mm thick block and tested at 4 K. The specimen fractured at the first serration and showed only 2 % elongation. Since the yield stress was 1279 MPa, the specimen did not show clear plastic deformation. A SEM image of the fracture surface and Nb distribution image are shown in Fig. 3. The fracture surface shows the ductile fracture but there are Nb segregation regions. From this result, it was recognized that the lower elongation was caused by the Nb segregation and special attention is necessary to produce the extra thick product.

As written above, all specimens in this study showed over 10 % elongation. When 100 mm thick block is focused, the elongation improves as the solution treatment temperature raises. It means that the higher temperature treatment promotes the Nb solid solution better, although the grain size becomes larger. The result shown in Fig. 3 reveals that there is a risk of segregation of Nb on the midsection of the bigger block.

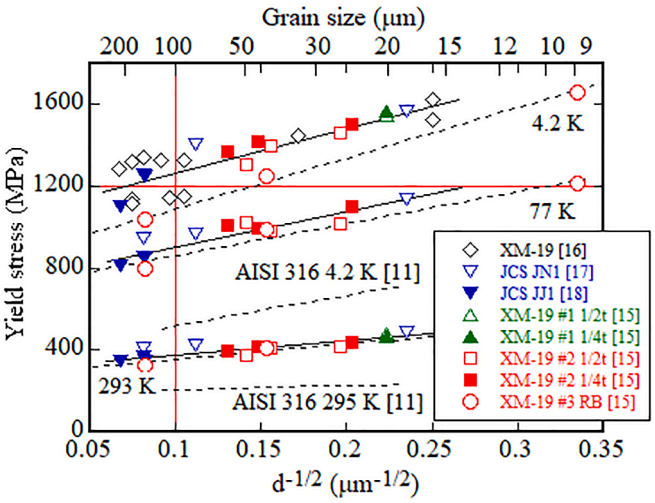

Fig. 4. Hall -Petch diagram of XM-19 and cryogenic structural materials.

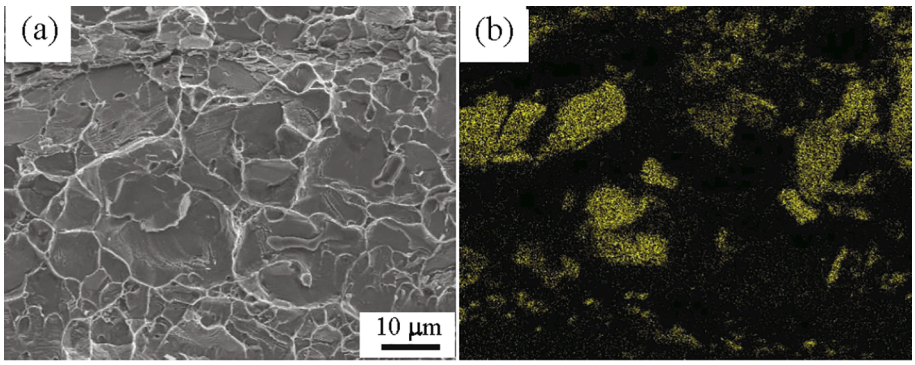

Fig. 3. (a) Fracture surface tested at 4 K and (b) Nb distribution image.

4.2. Hall-Petch diagram of cryogenic structural materials

The Hall-Petch diagram is shown in Fig. 4. The horizontal axis shows the parameter of $d^{-1/2}$, where d is an average grain size. Two dotted lines described as AISI 316 295 K and AISI 316 4.2 K show the results of 316 with very low N [11].

The relations of AISI 316 are presented as follows [11]:

$$\text{For } 295\text{K}; \sigma_Y = 735 \times d^{-1/2} + 310 \quad (3)$$

$$\text{For } 4\text{K}; \sigma_Y = 1505 \times d^{-1/2} + 363 \quad (4)$$

The yield stress of 316 at 4 K is around 600 MPa to 700 MPa. Since 316 does not contain much nitrogen, there is little solid solution strengthening, and the increment of the yield stress from room temperature to 4 K is not so large.

The data obtained in this research [15] are plotted together with the published data of XM-19 [16], and JCS JN1 [17] and JCS JJ1 [18]. Although some scatter is observed, it is very clear that the yield stress (σ_Y) increases as the grain size becomes smaller. The regression lines at each temperature with a solid line are presented as follows:

$$\text{For } 295\text{K}; \sigma_Y = 726 \times d^{-1/2} + 302 \quad (5)$$

$$\text{For } 77\text{K}; \sigma_Y = 1765 \times d^{-1/2} + 727 \quad (6)$$

$$\text{For } 4\text{K}; \sigma_Y = 2170 \times d^{-1/2} + 1046 \quad (7)$$

Because of the N solid solution strengthening, the yield stress at 4 K increases remarkably comparing with the room temperature. But the JCS JJ1 (N content; 0.21–0.27 mass %) and JCS JN1 (about 0.34 mass %) are also plotted on the same scatter band. So, it is recognized that the N solid solution strengthening effect is not linear. And there is a clear effect of the crystal refinement strengthening by Nb and V. On the other hand, the precipitation strengthening by V and Nb will be small because the results of XM-19 are in the same band with the results of JCS JJ1 and JCS JN1 which do not contain V and Nb. It should be noted that the yield stress of XM-19 and JCS materials mainly depends on the N solution strengthening and the grain size.

All steels presented in Fig. 4 have the nitrogen content of about 0.3 mass %. When the Eq. (2) is considered, the yield stress at 4 K will become over 1200 MPa in case that (C + N) is 0.3 mass %. Most of the data including the midsection strength except for the larger grains shown in Fig. 4 are plotted in the range of over 1200 MPa of the 4 K yield stress, and the (C + N) parameter is still available.

The results of #3 show the lower strength than those of #1 and #2 at every temperature. The regression lines with a dotted line at each temperature were obtained as follows:

$$\text{For } 295\text{K}; \sigma_Y = 726 \times d^{-1/2} + 280 \quad (8)$$

$$\text{For } 77\text{K}; \sigma_Y = 1582 \times d^{-1/2} + 698 \quad (9)$$

$$\text{For } 4\text{K}; \sigma_Y = 2423 \times d^{-1/2} + 857 \quad (10)$$

The nano scale precipitation of V and Nb interrupts the dislocation motion and increases the yield stress. Since #3 contains lower V and Nb, the nano scale precipitation effect becomes smaller resulting in the lower yield stress. Since the large-scale products are manufactured by the hot working, the Eqs. (5) to (7) are more important for the practical production. From these results, it seems that the higher yield stress at 4 K will be obtained by increasing the Nb and V contents at the midsection. However, the uniformity of these elements in the large-scale product must be achieved, otherwise the segregation occurs, and the elongation degrades drastically.

Since 316LN and JCS materials do not contain Nb and V in the matrix, the crystal refinement strengthening cannot be expected. The grain size control of these steels is carried out by controlling the strain hardening, the annealing temperature and the quenching procedure. Generally, such grain size control process is hard to apply to the huge blocks or the extra thick plates.

To achieve the targeted yield stress of 1200 MPa at the midsection, the grain size must be smaller than about 200 μm taking account of the lowest content of V and Nb, when XM-19 is supposed. Since the targeted yield stress is the design yield stress, all experimental data must exceed the targeted stress. So, it is better to set the target grain size to smaller than 100 μm. The grain size and the nano scale precipitation would be good reference for the development of the extra thick new cryogenic materials.

4.3. Toughness vs yield stress diagram

The fracture toughness based on the fracture mechanics is taken as the mechanical parameter to ensure the safety of the structure with cracks under the critical environment.

The diagram between the yield stress and the fracture toughness, $K_{IC}(J)$ and $K_Q(J)$, is shown in Fig. 5. There is a tendency that the toughness decreases when the yield stress increases as shown in NIST trend line for 300 series austenitic steels [19,11] which has about +/-30 MPa$\sqrt{m}$ scatter. All data obtained in this research [15] were invalid, $K_Q(J)$, because of the tunneling crack extension. The JAERI box, over 1200 MPa of yield stress and over 200 MPa$\sqrt{m}$ of toughness, was defined in 1980 s [7]. The ITER requirement box shows the required region for the ITER TF coil case material, which is over 1000 MPa of yield stress and over 200 MPa$\sqrt{m}$ of the toughness. A lot of mechanical tests of XM-19 were carried out for the tie rod of the ITER CS modules [16] as shown in Fig. 5 (Open round symbols). Depending on the manufacturing process, the product thickness, the steel vender, the toughness and the yield stress varied very widely, but the results provide the evidence of potential for what material can be produced by defining the manufacture conditions. The base metals, TIG weld joints and EBW joints of the JCS materials such as JCS JJ1, JCS JN1 and JCS JK1 are also plotted with triangle symbols [8]. The TIG weld joints (solid inverted triangle symbols) show the lower toughness than the base metal. Since the grain size and the precipitation of the inclusions in the weld metal vary widely, the wider welding conditions must be investigated for the practical application.

The dotted lines designated as "a = 1 mm" and "a = 5 mm" show the relation of $K_{IC} = \sigma_Y\sqrt{(\pi a)}$ which presents the critical fracture toughness of the crack with the length of 2a in an infinite plate when the yield stress is applied at infinity. When the maximum design stress is assumed $(2/3)\sigma_Y$, following ASME design code, the allowable crack length will be 9/4 times larger under the same K_{IC}, which means 11.25 mm instead of 5 mm in the figure, and it is a possible crack size to be detected by

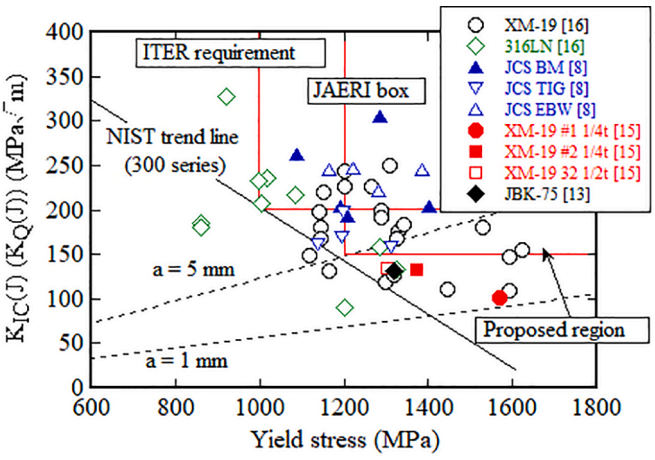

Fig. 5. Relation between yield stress and fracture toughness.

ultrasonic testing. Therefore, the region of over 1200 MPa and over 150 MPa$\sqrt{m}$ is proposed for the new cryogenic structural material.

The toughness obtained in this research [15] do not reach the 150 MPa$\sqrt{m}$, but it is expected that it can be performed by controlling the chemical compositions and the solution heat treatment conditions. Some data of XM-19 are plotted in the proposed region, and it is possible to produce the huge blocks satisfying the proposed region. The plot of JBK-75 shows the same level as the results obtained in this research. As shown in Table 1, it contains Ti and Mo to demonstrate the precipitation strengthening, and very low N. This material is one example of precipitation strengthening and almost no N solid solution strengthening.

Since the grain size in the midsection of the huge products tends to be large and the toughness would be lowered, it would be another reason that the fracture toughness as 150 MPa$\sqrt{m}$ would be the minimum for the design of a large-scale TF coil case.

4.4. Production and weldability

A lot of research and development works have been implemented to develop the cryogenic structural materials with high strength and high toughness at 4 K. As the results, there were several successes to satisfy the target of over 1200 MPa and 200 MPa$\sqrt{m}$ mainly by applying (C + N) solid solution strengthening. However, when the huge block was produced, it became clear that the midsection was weaker than the surface part. It raises difficulties in how to determine the design yield stress. Although one inch level thickness plate shows the high performance satisfying JAERI box, the extra thick plate such as 400 mm thick plate show the lower strength in the midsection. To improve the strength in the midsection of the huge block or extra thick plate, some investigations were carried out and 100 mm thick blocks of XM-19 were trial produced in this research.

Generally, EBW joint would show the high yield stress and high toughness. All EBW joint data in Fig. 5 (Open triangle symbol) show over 200 MPa$\sqrt{m}$, but the plate thickness was not clear. The TIG joint would show the relatively lower toughness. All TIG joint data in Fig. 5 (inverted triangle symbol) show the toughness of in between 150 MPa$\sqrt{m}$ and 200 MPa$\sqrt{m}$. During the TIG welding, the nitrogen would be released and decreased in the weld metal, and the grain size would be larger than the base metal. For the EBW, high N content is not welcome because of high possibility of the porosity formation. In case of the TIG welding with a narrow groove, the bubbling of N in the molten pool could be controlled by the smaller heat input and the slower welding speed, although they are not high efficiency welding conditions. Therefore, too much N content like 0.3 mass % must be considered. As shown in Fig. 4, there are the clear crystal refinement strengthening and the nano scale precipitation strengthening by adding V and Nb. So, there will be potential to reduce N content to around 0.2 mass % to make the welding easier. When the JBK-75 is taken up, it shows the precipitation strengthening and almost no effect of the N solid solution strengthening. The Ti and Mo precipitation effect must be investigated more carefully, and the proper content range of N must be defined to improve the midsection strength of the huge wrought products.

Since the heat treatment condition is a key parameter to realize both strengthening effects, the temperature history at the midsection of huge wrought product would be investigated. If the proper heat treatment profile could be determined, the trial production will be meaningful using the partial water quenching or the oil quenching.

5. Summary

The fusion DEMO design is in progress conceptually, and it is supposed that the huge wrought would be necessary to support the huge electromagnetic force. In parallel, some challenging projects to realize D-T reaction such as SPARC are undergoing, and the operation temperature seems to be about 20 K. To support the huge electromagnetic force, the yield stress at the midsection of the large wrought is anticipated to be the same as that at the surface area.

In this paper, the development policy for the extra thick new cryogenic structural material was discussed focusing on the mechanical properties at the midsection of the extra thick plate or block and presenting some data at 4 K of the trial-manufactured thick XM-19 together with the published data.

The main results are summarized as follows:

(1) Although the (C + N) solid solution strengthening has been applied to increase the strength at the cryogenic temperatures, the crystal refinement strengthening and the nano scale precipitation strengthening by the V and Nb are good methods to improve the yield stress at the midsection of the extra thick plate.
(2) The Nb segregation must be avoided, because the elongation drops drastically. Since there is no non-destructive detection method of segregation, careful work must be performed during the steelmaking process.
(3) The solution heat treatment condition is very important to generate the high performance of the strengthening process at the midsection of the big wrought. The monitoring of the temperature history would be one process to maintain the expected process.
(4) To perform the welding effectively, it is preferable to reduce the N content to around 0.2 mass % which is the same level as 316LN.

CRediT authorship contribution statement

Arata Nishimura: Supervision, Data curation, Resources, Investigation, Conceptualization. **Yoshinori Ono:** Data curation, Resources, Investigation, Conceptualization. **Osamu Umezawa:** Data curation, Resources, Investigation, Conceptualization. **Susumu Kumagai:** Data curation, Resources, Investigation, Conceptualization. **Yohko Kato:** Writing – original draft, Investigation. **Tetsuya Kato:** Writing – original draft, Data curation, Investigation. **Tetsumi Yuri:** Data curation, Investigation. **Masayuki Komatsu:** Data curation, Investigation.

Declaration of Competing Interest

The authors declare that they have no known competing financial interests or personal relationships that could have appeared to influence the work reported in this paper.

Acknowledgement

Part of the work was supported by the framework of the Joint Special Design Team for Fusion DEMO contract research program of National Institutes for Quantum and Radiological Science and Technology in Japan and the NIFS Collaborative Research Program (NIFS19KERF048 and NIFS19KECF029).

References

[1] ITER web site. https://www.iter.org/.
[2] K. Tobita, N. Asakura, R. Hiwatari, Y. Someya, H. Utoh, K. Katayama, A. Nishimura, Y. Sakamoto, Y. Homma, H. Kudo, Y. Miyoshi, M. Nakamura, S. Tokunaga, A. Aoki, the Joint Special Design Team for Fusion DEMO, "Design strategy and recent design activity on Japan's DEMO", Fusion Sci. Technol. 72 (4) (2017) 537–545, https://doi.org/10.1080/15361055.2017.1364112.
[3] G. Federici, C. Bachmann, L. Barucca, W. Biel, L. Boccaccini, R. Brown, C. Bustreo, S. Ciattaglia, F. Cismondi, M. Coleman, V. Corato, C. Day, E. Diegele, U. Fischer, T. Franke, C. Gliss, A. Ibarra, R. Kembleton, A. Loving, F. Maviglia, B. Meszaros, G. Pintsuk, N. Taylor, M.Q. Tran, C. Vorpahl, R. Wenninger, J.H. You, DEMO design activity in Europe: Progress and updates, Fusion Eng. Des. 136 (2018) 729–741, https://doi.org/10.1016/j.fusengdes.2018.04.001.
[4] A. Nishimura, Study on Assembly of TF Coil and Vacuum Vessel for Fusion DEMO, Plasma Fusion Res. 16 (2021), https://doi.org/10.1585/pfr.16.2405036.
[5] D.G. White, J. Minervini, B. LaBombard, E. Marmar, L. Bromberg, M. Greenwald, Smaller & Sooner: Exploiting High Magnetic Fields from New Superconductors for

a More Attractive Fusion Energy Development Path, J. Fusion Energy 35 (2016) 41–53, https://doi.org/10.1007/s10894-015-0050-1.
[6] Plasma Science and Fusion Research Center, MIT, web site. https://www.psfc.mit.edu/sparc.
[7] H. Nakajima, K. Yoshida, S. Shimamoto, Development of new cryogenic steels for the superconducting magnets of the Fusion Experimental Reactor, ISIJ Int. 30 (8) (1990) 567–578.
[8] H. Nakajima, H. Tsuji, Development and Prospects of Material Technology in Superconducting Coils for Fusion Reactor, J. Plasma Fusion Res. 70 (1994) 733–739, in Japanese.
[9] K. Hamada, Cryogenic structural material, J. Plasma Fusion Res. 83 (2007) 33–38, in Japanese.
[10] The Japan Society of Mechanical Engineers. Code for Fusion Facilities. Rules on Superconducting Magnet Structure, JSME SKA1-2013.
[11] K.D. Timmerhaus, R.P. Reed, Cryogenic Engineering - Fifty Years of Progress -, Springer, 2019.
[12] K. Okuno, H. Nakajima, N. Koizumi, From CS and TF Model Coils to ITER: Lessons Learnt and Further Progress, IEEE Trans. Appl. Supercond. 16 (2) (2006) 880–885, https://doi.org/10.1109/TASC.2006.873317.
[13] R.E. Gold, W.A. Logsdon, G.E. Grotke, B. Lustman, Evaluation of conductor sheath alloys for a forced-flow Nb_3Sn superconducting magnet coil for the large coil program, Adv. Cryog. Eng. 28 (1982) 759–770.
[14] K.D. Freudenberg, R.L. Myatt, ITER central solenoid support structure analysis, in: IEEE/NPSS 24th Symp. on Fusion Eng., 2011, https://doi.org/10.1109/SOFE.2011.6052298.
[15] T. Kato, Y. Kato, O. Umezawa, Y. Ono, A. Nishimura, S. Kumagai, T. Yuri, Tensile properties of XM-19 austenitic stainless steel thick plates and bars at cryogenic temperatures, IOP Conference Series: Materials Science and Engineering. To be submitted.
[16] D.M. McRae, S. Balachandran, R.P. Walsh, Fatigue and fracture of three austenitic stainless steels at cryogenic temperatures, IOP Conf. Ser.: Mater. Sci. Eng. 279 (2017) 012001, https://doi.org/10.1088/1757-899X/279/1/012001.
[17] K. Suemune, T. Sakamoto, T. Ogawa, et al., Manufacture and properties of nitrogen-containing Cr-Mn and Cr-Ni austenitic stainless steels for cryogenic use, Adv. Cryog. Eng. 34 (1998) 123–129.
[18] J. Ishizaka, R. Miura, S. Shimamoto, H. Nakajima, Strength and Toughness of 12Cr-12Ni-10Mn-5Mo Steel for Cryogenic Structural Application, Tetsu Hagane 76 (5) (1990) 791–798.
[19] R.L. Tobler, A. Nishimura, J. Yamamoto, Design-relevant Mechanical Properties of 316-type Steels for Superconducting Magnets, Cryogenics 37 (9) (1997) 533–550.